Maria Pellegrini,[1,2]
Marina Gobbo,[2]
Raniero Rocchi,[2]
Evaristo Peggion,[2]
Stefano Mammi,[2]
Dale F. Mierke[1,3]

[1] *Gustaf H. Carlson School of Chemistry, Clark University, 950 Main Street, Worcester, MA 01610, USA*

[2] *Department of Organic Chemistry, University of Padova, Biopolymer Research Center, Via Marzolo 1, Padova, Italy, I-35131*

[3] *Department of Pharmacology and Molecular Toxicology, University of Massachusetts, Medical Center, 55 Lake Avenue North, Worcester, MA 01655, USA*

Threonine^6-Bradykinin: Conformational Study of a Flexible Peptide in Dimethyl Sulfoxide by NMR and Ensemble Calculations

Received 15 August 1996; accepted 20 November 1996

Abstract: *The conformation of the natural peptide threonine^6 (Thr^6)-bradykinin, Arg^1-Pro^2-Pro^3-Gly^4-Phe^5-Thr^6-Pro^7-Phe^8-Arg^9, was investigated in DMSO by nmr spectroscopy and computer simulations. The structural analysis of the Thr^6-peptide is made particularly interesting by the fact that despite the high sequence homology with native bradykinin (only one conservative substitution: Ser^6/Thr^6) there is a marked and significant difference in the biological profiles of the two peptides.*

The nmr spectra indicate a relatively flexible structure with the presence of an N-terminal turn. Standard distance geometry calculations failed to produce structures in accord with the experimental observations; the resulting structures are indeed too rigid and conformationally restricted for the nmr data. The results of ensemble calculations reveal conformational changes occurring rapidly on the nmr time scale and allow for the establishment of a series of disordered conformations, prevalently extended with a partially populated turn in residues 2–5, which when considered together, as an average, fulfill the experimental restraints. The structural characterization of (Thr^6)-bradykinin supports the hypothesis of the significant role of the residue at position 6 on both conformation as well as biological activities and suggests a N-terminal turn as a possible bioactive conformation. © *1997 John Wiley & Sons, Inc. Biopoly* ***40:*** *561–569, 1996*

Keywords: *bradykinin; nmr; peptide conformation; ensemble averages; distance geometry calculations*

Correspondence to: Dale F. Mierke, Gustaf H. Carlson School of Chemistry, Clark University, 950 Main Street, Worcester, MA 01610, USA

CCC 0006-3525/97/050561-09

INTRODUCTION

Bradykinin (BK; Arg[1]-Pro[2]-Pro[3]-Gly[4]-Phe[5]-Ser[6]-Pro[7]-Phe[8]-Arg[9]), a linear nonapeptide, is a plasma and tissue hormone released upon tissue injury or trauma by the proteolytic action of kallicreins on kininogens.[1] The peptide is implicated in numerous pathophysiological processes. BK elicits contraction or relaxation of vascular smooth muscles as well as increased vascular permeability that leads to edema[2,3] and produces contraction of smooth muscles in different organs.[4] BK is also responsible for the cardinal symptoms of inflammation[5] and in the nervous system it is very important for initiation of pain stimuli.[6] BK is also tentatively associated with symptoms of the common cold.[7,8]

The conformational analysis of BK, BK fragments, and analogues is the object of considerable interest—the aim of which is to gain insight into a possible bioactive conformation and develop a structure activity relationship. The general conclusion of conformational studies in aqueous solution is that BK exists in many conformational states.[9] However, in alternative solvent systems the nonapeptide prefers folded conformations. Cann and coworkers[10] reported that the conformation of bradykinin in dimethyl sulfoxide (DMSO) contains two sequential β-turns, about residues 5–8 and 6–9. A more recent study of BK in DMSO[11] identified a β-turn of type III (Ser[6]–Arg[9]), although this conformation was generated by the use of a questionable hydrogen-bond constraint. The problems associated with the use of hydrogen-bond restraints in small peptides has been addressed in the literature.[12] A β-turn has also been observed in dioxane : water (9 : 1), lyso phosphatidylcholine micelles, and sodium dodecylsulfate (SDS) micelles.[13] The results from these conformational investigations, along with the studies of peptidic agonists and antagonists, has led to the hypothesis that a β-turn in the four C-terminal amino acids is a prerequisite for activity and that the type of β-turn adopted is related to the difference between agonist and antagonist, together with the required orientation of the side chains.[14–19]

In the studies described above, the N-terminal portion of BK is conformationally flexible. The only exception is in trifluoroethanol : water (TFE/H_2O 95/5% v/v)[20] in which BK adopts an N-terminal turn, involving residues 1–4 and a *cis* peptide bond between Pro[2] and Pro[3]. Similar turns have also been observed for cyclic bradykinins.[21] The N-terminal β-turn has been frequently observed in BK antagonists with a hydroxyproline in position 3.[22,23] The turn, centered about Hyp[3]-Gly[4] and involving all *trans* bonds, was associated with the antagonistic activity.

Threonine[6] (Thr[6])-bradykinin, (Thr[6])-BK, was discovered in the venom of a solitary wasp[24] in 1983. The wasp stings its prey in all nerve ganglia involved in locomotion, resulting in irreversible paralysis; the effect has been explained as an immediate and permanent block of transmission at the presynaptic level.[25] In the insect central nervous system (CNS) (Thr[6])-BK proved to be 10 times more potent than BK, despite the single conservative substitution in the sequence.[26,27] The presence of (Thr[6])-BK and other BK-like peptides in wasp and ant venom and in frog skin suggests a toxic effect also in vertebrates, although the mode of action on mammalian CNS is still obscure.[25]

The peptide has been tested for the capability of stimulating smooth muscle contraction and the results have been compared with the ones for BK. Its potency in causing the contraction of the guinea pig rectum is 10 times higher than for BK, tested in the same experiment.[28]

In this study the peptide has been investigated in DMSO solution by nmr spectroscopy and distance geometry calculations, with the aim of developing high quality three-dimensional structures and assess the conformational preferences of the peptide. The existence of previous studies of BK in the same solvent system offered the possibility of comparisons between the two peptides and leading to an understanding, on a structural basis, of the differences in activity observed between BK and (Thr[6])-BK.

One problem in the determination of conformation from nmr data is the possibility of large, significant conformational changes fast on the nmr time scale. The nmr observables and the restraints developed from them will be consistent with an average structure that may not exist in solution or that is not even physically possible. The idea of "the structure" is no more suitable and an ensemble of conformations must be taken into account to explain the experimental data. (Thr[6])-BK is a small linear peptide, therefore expected to be flexible in solution. The application of the approach of ensemble calculations in the structure refinement from nmr data revealed to be determinant for a correct interpretation of the experimental restraints and to obtain a correct picture of the peptide conformation in DMSO solution.

EXPERIMENTAL METHODS

Nuclear Magnetic Resonance

The nmr experiments have been carried out on a 6 m*M* sample (based on weight) in DMSO-d_6 (Cambridge Iso-

Table I Proton Chemical Shifts (Referenced to the Solvent Peak, 2.49 ppm, T = 298 K), HN-H$^{\alpha}$ Coupling Constants and HN Temperature Coefficients of (Thr^6)-BK in DMSO-d_6

Residue	HN	Hα	Hβ	Hγ	Others	J (Hz)	$\Delta\delta/\Delta T$ (−ppb/K)
Arg[1]	8.14	4.17	1.68; 1.70	1.60	δ: 3.09 εNH: 7.68		
Pro[2]		4.59	1.83; 2.23	1.83; 1.92	δ: 3.71		
Pro[3]		4.25	1.82; 1.99	1.92	δ: 3.62		
Gly[4]	7.96	3.63					3.2
Phe[5]	7.92	4.63	2.74; 2.94		Ar: 7.18	8.7	3.9
Thr[6]	8.20	4.42	3.89	1.10	OH: —	7.6	7.8
Pro[7]		4.33	1.70; 1.90	1.57; 1.70	δ: 3.58		
Phe[8]	7.79	4.51	2.79; 3.03		Ar: 7.26	8.75	4.2
Arg[9]	8.19	4.20	1.60; 1.76	1.50	δ: 3.10 εNH: 7.59	7.55	5.1

topes). Proton spectra were recorded on a Bruker AM400 and on a Varian Unity 500 MHz spectrometer, and processed using a workstation X-32 (UXNMR software), Varian VNMR software or *Felix* (Biosym Technologies Inc., San Diego). Chemical shifts were calibrated with respect to the solvent resonance (2.49 ppm).

For assignment of the spin systems double quantum filtered correlated spectroscopy (COSY),[29] total COSY (TOCSY),[30,31] and nuclear Overhauser effect spectroscopy (NOESY)[32,33] spectra were recorded in the phase-sensitive mode using the time proportional phase incrementation method[34,35] (for the Bruker instrument) or the method from States et al.[36] (for the VARIAN instrument). A ROESY[37] spectrum with a mixing time of 200 ms was recorded in order to identify exchange phenomena for HN-HN and H$^{\alpha}$-H$^{\alpha}$ cross peaks of the NOESY spectrum; a spin–lock field of 2500 Hz was realized with a continuous wave, low power pulse. NOESY spectra were collected at 298 K with mixing times varying from 100 to 200 ms. The typical spectral width was in all cases of 4800 Hz in both dimensions, with 2048 data points in t_2 and 512 data points in t_1, and with 32–128 scans at each increment. Forward linear prediction to 1024 points and zero filling to 2048 were applied to the incremented dimension, Gaussian apodization was used in both t_2 and t_1.

The temperature coefficients were measured with TOCSY spectra (4096 points in t_2, 256 in t_1, and 4 scans per increment) recorded at temperatures between 298 and 313 K, by increments of 5 K. The proton assignments are given in Table I.

For determination of homonuclear coupling constants, the P.E. COSY[38] pulse sequence was employed. The spectrum was acquired at 298 K with 4096 data points in t_2 and 640 incremental data points. The t_2 dimension was expanded with zero filling to 8192 points.

Cross-peak volumes from the 200 ms NOESY spectrum were obtained using *Felix*, within the *Insight II* suite of programs (Biosym Technologies Inc., San Diego). The volumes were converted to distances using the isolated two-spin approximation and utilizing the cross peaks between the two β-methylene protons of the two Phe residues as a reference (1.78 Å). No evidence of spin diffusion was observed up to a mixing time of 200 ms. The distances were adjusted by ±10% to produce the upper and lower distance restraints (Table II). Pseudo atoms were used for aromatic protons, for methyl groups, and for methylene that could not be stereospecifically assigned, with the appropriate correction of the upper distance restraint following standard procedures.[39]

The HN-H$^{\alpha}$ coupling constants, utilized as restraints in the calculations, were measured from one-dimensional (1D) spectra, where possible, or from the P.E. COSY spectrum, following the procedure of Kim and Prestegard[40] to compensate for errors arising from line broadening.

Distance Geometry

The distance geometry calculations were carried out using a home-written program utilizing the random metrization algorithm of Havel.[41] Experimentally determined distances that were more restrictive than the geometric distance bounds (holonomic restraints)[42] were added to create a distance matrix. The structures were first embedded in four dimensions and then partially minimized using conjugate gradients followed by distance and angle driven dynamics (DADD).[43,44] The DADD simulation was carried out at 1000 K for 50 ps and then there was a gradual reduction in temperature over the next 30 ps. The DADD procedure utilizes the holonomic and experimental distance constraints plus a chiral penalty function for the generation of the violation "energy" and forces. The resulting structures were then reduced to three dimensions using metrization, and the optimization and DADD procedure repeated.

The following ensemble calculations are identical to those used for the DADD method, except that the penalty expression for the experimental restraints (NOEs and

Table II Interproton Distances (Upper Limits) Utilized in the Distance Geometry Calculations of (Thr^6)-BK in DMSOd_6

Atom 1		Atom 2		Distance (Å)	
Arg^1	HN	Arg^1	H_α	2.78	
	HN	Arg^1	$_\beta CH_2$	4.06	
	HN	Arg^1	$_\gamma CH_2$	4.60	
	HN	Arg^1	$_\delta CH_2$	4.46	
	$_\beta CH_2$	Arg^1	H_ϵ	5.07	
	H_α	Pro^2	$_\delta CH_2$	3.38	
Pro^2	H_α	Pro^3	$_\delta CH_2$	3.52	
Pro^3	H_α	Gly^4	HN	3.00	
	H_α	Phe^5	HN	3.78	$i, i+2$
Gly^4	HN	Gly^4	$_\alpha CH_2$	3.05	
	$_\alpha CH_2$	Phe^5	HN	3.32	
Phe^5	HN	Phe^5	H_α	3.02	
	HN	Phe^5	H_β^{ProR}	2.82	
	HN	Phe^5	H_β^{ProS}	3.37	
	H_α	Phe^5	H_β^{ProR}	2.93	
	H_α	Phe^5	H_β^{ProS}	2.77	
	H_{ar}	Phe^5	H_α	5.59	
	H_{ar}	Phe^5	H_β^{ProR}	5.37	
	H_{ar}	Phe^5	H_β^{ProS}	5.46	
	H_{ar}	Thr^6	$_\gamma CH_3$	8.70	
	H_α	Thr^6	HN	2.37	
	H_β^{ProS}	Thr^6	HN	3.48	
	HN	Thr^6	HN	3.43	
Thr^6	HN	Thr^6	H_α	3.16	
	HN	Thr^6	H_β	2.87	
	HN	Thr^6	$_\gamma CH_3$	4.31	
	H_α	Thr^6	H_β	2.80	
	H_α	Thr^6	$_\gamma CH_3$	4.21	
	H_β	Thr^6	$_\gamma CH_3$	3.51	
	H_α	Pro^7	$_\delta CH_2$	3.45	
	$_\gamma CH_3$	Pro^7	$_\delta CH_2$	5.08	
	$_\gamma CH_3$	Phe^8	HN	5.21	$i, i+2$
Pro^7	H_α	Phe^8	HN	2.40	
	H_β^{ProR}	Phe^8	HN	3.79	
	H_β^{ProR}	Phe^8	H_{ar}	6.20	
Phe^8	HN	Phe^8	H_α	2.88	
	HN	Phe^8	H_β^{ProR}	2.81	
	HN	Phe^8	H_β^{ProS}	3.69	
	H_α	Phe^8	H_β^{ProR}	3.79	
	H_α	Phe^8	H_β^{ProS}	2.77	
	H_{ar}	Phe^8	H_α	5.73	
	H_{ar}	Phe^8	H_β^{ProR}	5.57	
	H_α	Arg^9	HN	2.37	
	H_β^{ProS}	Arg^9	HN	3.30	
	HN	Arg^9	HN	3.27	
Arg^9	HN	Arg^9	H_α	3.16	
	HN	Arg^9	$_\gamma CH_2$	4.59	
	HN	Arg^9	$_\delta CH_2$	4.66	
	H_α	Arg^9	$_\beta CH_2$	3.41	
	H_α	Arg^9	$_\gamma CH_2$	4.67	

coupling constants)[12,44] and the forces calculated from these restraints are generated from an ensemble average. The ensemble calculations utilized 10,000 steps of 0.01 ps at 500 K, followed by a slow reduction of the temperature to 1 K for 2500 steps. The metrization and refinement of 100 structures required approximately 15 h of cpu using a single processor on a SGI Indigo2 (R4400) for the classical distance geometry (DG), and about one week for the ensemble calculations. Energy minimization and interactive modeling were performed using *Discover* (Consistent Valence Force Field, CVFF91) and *Insight II* (Biosym Technologies Inc., San Diego). Analyses of the structures in terms of rms deviation (rmsd) values and dihedral angle distribution were performed using home-written programs.

RESULTS AND DISCUSSION

The ^{1}H-nmr spectra revealed the presence of more than one configurational isomer in solution, in slow equilibrium on the nmr time scale. The complete spin systems of all the residues could only be assigned for the major configurational isomer, and therefore only it is considered further here. The relative intensities of the resolved peaks in a 1D ^{1}H spectrum indicate that this isomer is present in a 9 : 1 ratio relative to the second most populated species. The different isomers originate from *cis*/*trans* isomerization at the three X-Pro bonds and exchange cross peaks were identified in a rotating frame NOESY spectrum.

The major isomer has a *trans* configuration at all of the prolines, as determined from diagnostic $H_i^{\alpha}/H_{i+1}^{\delta 1}$ and $H_i^{\alpha}/H_{i+1}^{\delta 2}$ cross peaks between the proline residues and the preceding amino acids in the NOESY spectra. Stereospecific assignments for three prochiral centers (position β of Phe 5 and 8 and of Pro 7) obtained from the analysis of NOESY and P.E. COSY spectra were used in the calculations.

A total of 50 NOEs have been observed and the upper distance limits derived from these observations used in the calculations are listed in Table II. Of these, most are sequential or intraresidue. An expanded portion of the amide to aliphatic region of a NOESY spectrum illustrating strong sequential connectivities $H_i^{\alpha}-HN_{i+1}$ is shown in Figure 1. The only evidence of a folded conformation in this region of the spectrum is a $H_i^{\alpha}-HN_{i+2}$ cross peak between Pro^3 and Phe^5. Such $\alpha N(i, i+2)$ NOEs are normally interpreted as arising from β-turn structures.[45-47] In the amide region two HN_i/HN_{i+1} connectivities have been assigned to Phe^5/Thr^6 and Phe^8/Arg^9. The presence of strong sequential connectivities (the strongest cross peaks in this region of the spectrum) and the weak $\alpha N(i, i+2)$ NOE suggests a prevalently disordered molecule in solution with a possible bend at the N-terminus. The amide temperature coefficients can usually help in identifying β-turn structures, allowing for the recognition of amide protons involved in hydrogen bonds. However, no temperature coefficients lower than 3 ppb/K were measured, a further indication of conformational flexibility (the lowest values were 3.2 and 3.9, belonging to Gly^4 and Phe^5, respectively). To better characterize the conformation(s) of (Thr^6)-BK in solution and the extent of conformational order, distance geometry calculations were carried out.

The DG calculations produced 90 low energy structures. The structures were analyzed in terms of violations of the experimental restraints (NOEs and coupling constants), distribution of backbone dihedral angles ϕ and ψ, and pairwise rmsd. The resulting DG structures are structured at both termini, with high flexibility centered at the sixth residue (Thr), acting as a hinge. This is clearly shown in Figure 2 where 50 DG structures (only 50 structures are shown for clarity) are superimposed utilizing backbone heavy atoms in the N-terminus (Pro^2–Phe^5, shown in panel A) and C-terminus (Pro^7–Arg^9, displayed in panel B). From the rmsd values, ϕ, ψ dihedral angles, and simply viewing the DG structures, the conformations are far too refined; a level of refinement that cannot be justified by the NOEs data, which as described above are mainly intraresidue and sequential.

A clue to the problem was obtained from detailed analysis of the violations of the experimental restraints. Although the coupling constant ($^3J_{HN-H\alpha}$) restraints were fulfilled, there were problems in fulfilling specific interproton distances. One of the short, sequential upper limit distances ($H_i^{\alpha}-HN_{i+1}$) was significantly violated (approximately 0.4 Å) in all of the 90 structures. Interestingly, it was not the same $H_i^{\alpha}-HN_{i+1}$ NOE that was violated in every structure. Moreover, a short distance was always observed between Gly^4_{HN} and Phe^5_{HN} (2.4 Å on average over the 90 structures), while no NOE was observed between these protons (these two protons are highlighted in gray in Figure 2, top). A new DG calculation was carried out imposing a lower bound of 3.5 on this proton pair (non-NOE). However, this calculation led to distorted structures with an additional large violation of the NOE between $Pro^3_{H\alpha}$ and Gly^4_{HN}.

One reason for the discrepancy between the calculated structures and the experimental data could be conformational exchange fast on the nmr time

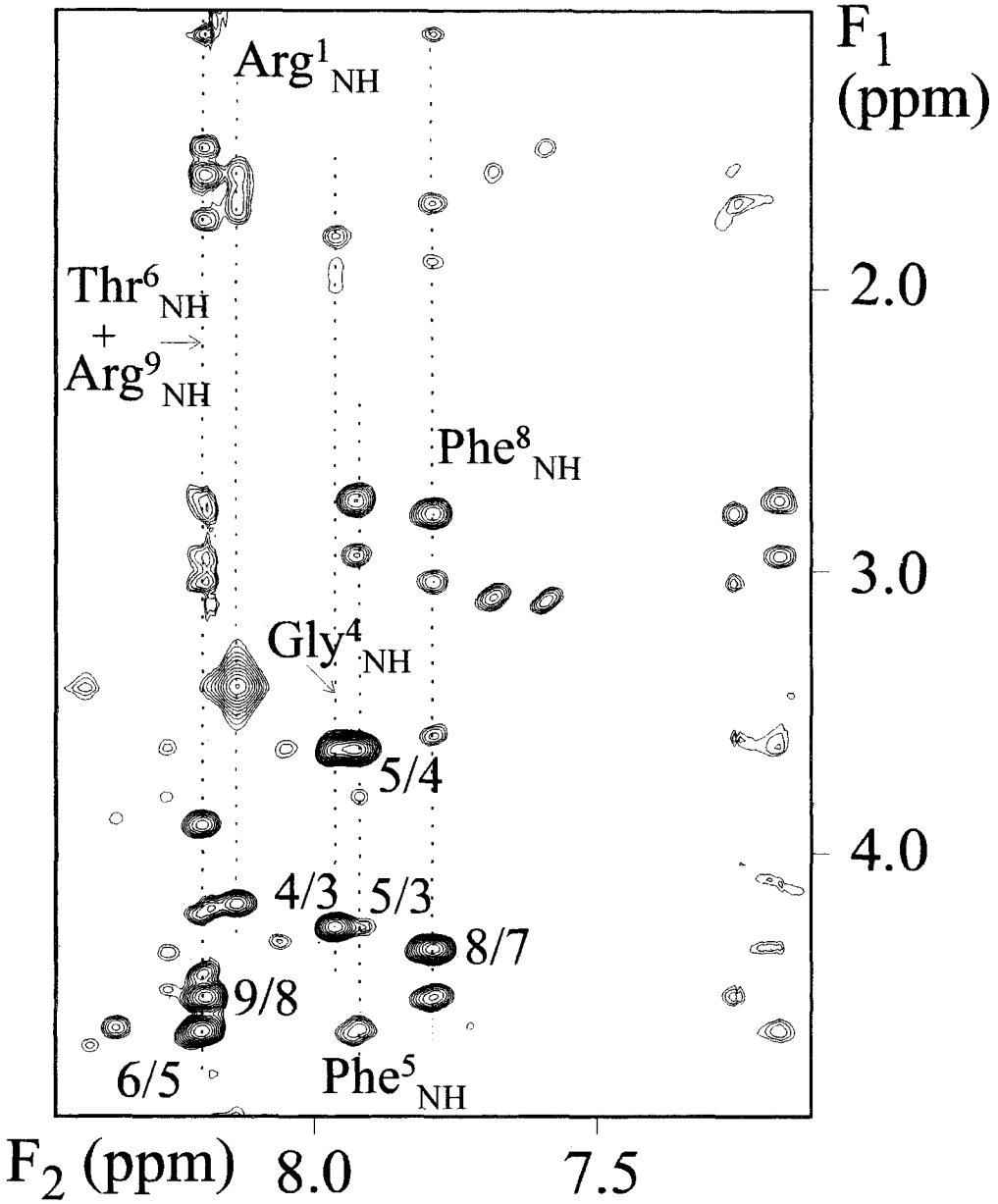

FIGURE 1 Expanded portion of a NOESY spectrum of (Thr^6)-BK in DMSO solution (mixing time = 200 ms, T = 298 K). The resonances of the amide protons and some relevant NOEs are labeled.

scale. In the presence of such dynamics, the nmr observables (NOEs and coupling constants) are averaged quantities and must be handled as such during the computational refinement; the constraints generated from averaged NOE cannot be fulfilled by one structure. Therefore, ensemble simulations that utilize a large number, an ensemble, of structures were carried out. The 90 DG structures copied 5 times constituted the starting ensemble. This is indeed a distorted starting ensemble (i.e., the structures are clustered in the region of conformational space allowed by the experimental restraints in the classical "one-structure" DG calculations). A nonbiased starting ensemble could be generated by DG calculations using no restraints. However, this should not be necessary given the fact that previous simulations indicate that the ensemble protocol allows the structures to overcome local energy barriers and sample all conformational space (a uniform and complete sampling of the ϕ, ψ space).[48]

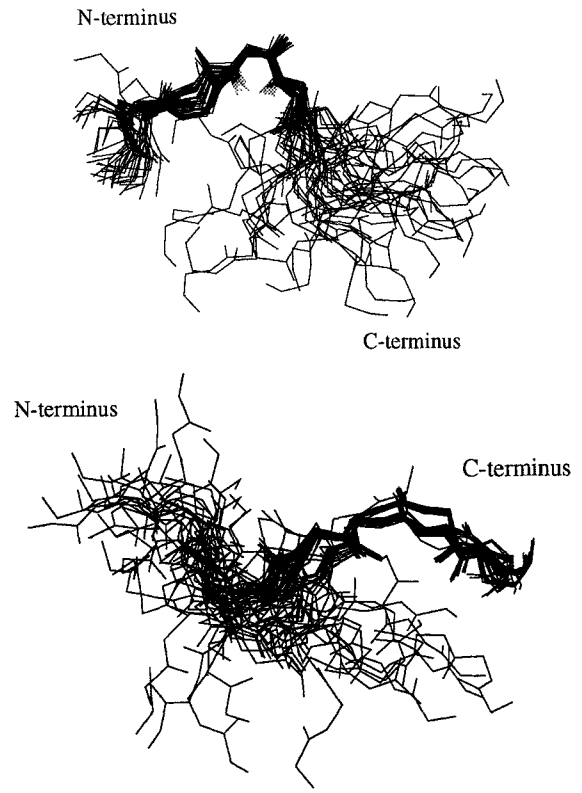

FIGURE 2 Superposition of 50 low energy structures obtained from distance geometry calculations. The structures are superimposed using the heavy backbone atoms of residues 2–5 (top) and residues 7–9 (bottom). Only backbone atoms are shown for clarity, with the exception of the amide protons of Gly^4 and Phe^5, which are depicted in grey.

In the ensemble simulations only the average over all the structures (450 structures) is required to fulfill the experimental restraints; this naturally accounts for fast conformational averaging occurring in solution. No violations to upper or lower distance restraints greater than 0.1 Å were observed in the resulting structures, including the short sequential distances, the NOE between $Pro^3_{H\alpha}$ and Phe^5_{HN}, and the distance between Gly^4_{HN}/Phe^5_{HN}, discussed above. Results from the ensemble calculation in the form of ϕ, ψ maps are shown in Figure 3. The region of the Ramachandran maps obtained from the classical one-structure DG are shown for comparison. The conformational space populated by the structures obtained from the ensemble calculations is clearly larger.

The results for Pro^3–Gly^4 indicate a prevalently extended conformation; however, approximately 20% of the population is consistent with a β-turn structure (either type I or II, allowing a ±20° deviation from standard values). This turn is expected according to Wilmot and Thorton's predictions[49] of Pro in position $(i + 1)$ as the most strongly preferred amino acid for both type I and II β-turns. Furthermore, on the basis of Chou and Fasman's analysis,[50] the sequence Pro^2-Pro^3-Gly^4-Phe^5 has a significant β-turn probability.

The results of the conformational preferences of (Thr^6)-bradykinin find some antecedent in the conformational study of α-methyl proline containing BK analogues. Evidence of an N-terminal β-turn in positions 2–5 was reported by Welsh et al.,[51] who examined BK analogues substituted in position 3 or 7 with α-MePro in aqueous solution. The formation of turns at the N-terminus (2–5) and at the C-terminus (6–9) was hypothesized to be cooperative, since the substitution of only one of the prolines with α-MePro induces a turn also in the other position. The other report of an N-terminal β-turn involved a BK antagonists with hydroxyproline in position 3 and D-amino acid in position 7.[22,23] The D-amino acid in position 7 is essential for antagonistic activity while the Hyp^3 increases selectivity and potency. One of the most potent of these antagonists, Hoe 140, studied in water and SDS micelles displays both a C-terminal βII′-turn (6–9) and an N-terminal βII-turn (2–5).[23]

BK and (Thr^6)-BK, despite the single conservative substitution (Ser → Thr), display different activities at a common receptor, which may be correlated to the differences observed for their conformational preferences. In DMSO solution, the peptides display distinct conformational features. In water and in the presence of SDS micelles,[52] (Thr^6)-BK shows a greater tendency to adopt a β-turn of type I or II in the C-terminus, when compared to BK studied under similar conditions. This difference, an effect of the substitution at position 6, is in accord with the observation of cooperativity in the process of folding for the α-MePro analogues and the importance of a N-terminal turn in the bioactive conformation.

The natural peptide (Thr^6)-BK has been examined in DMSO by nmr and distance geometry calculations. (Thr^6)-BK is a short linear peptide and naturally conformationally flexible in solution. The nmr observables are an average of the different conformations interconverting fast on the nmr time scale. The ensemble approach utilized in the structure refinement step allowed for the determination of the species present in solution as mainly disordered structures with a tendency of the N-terminus to adopt a turn centered about Pro^3–Gly^4. This secondary structure element was not observed for BK and therefore must be a result of the substitution at position 6. We attribute the

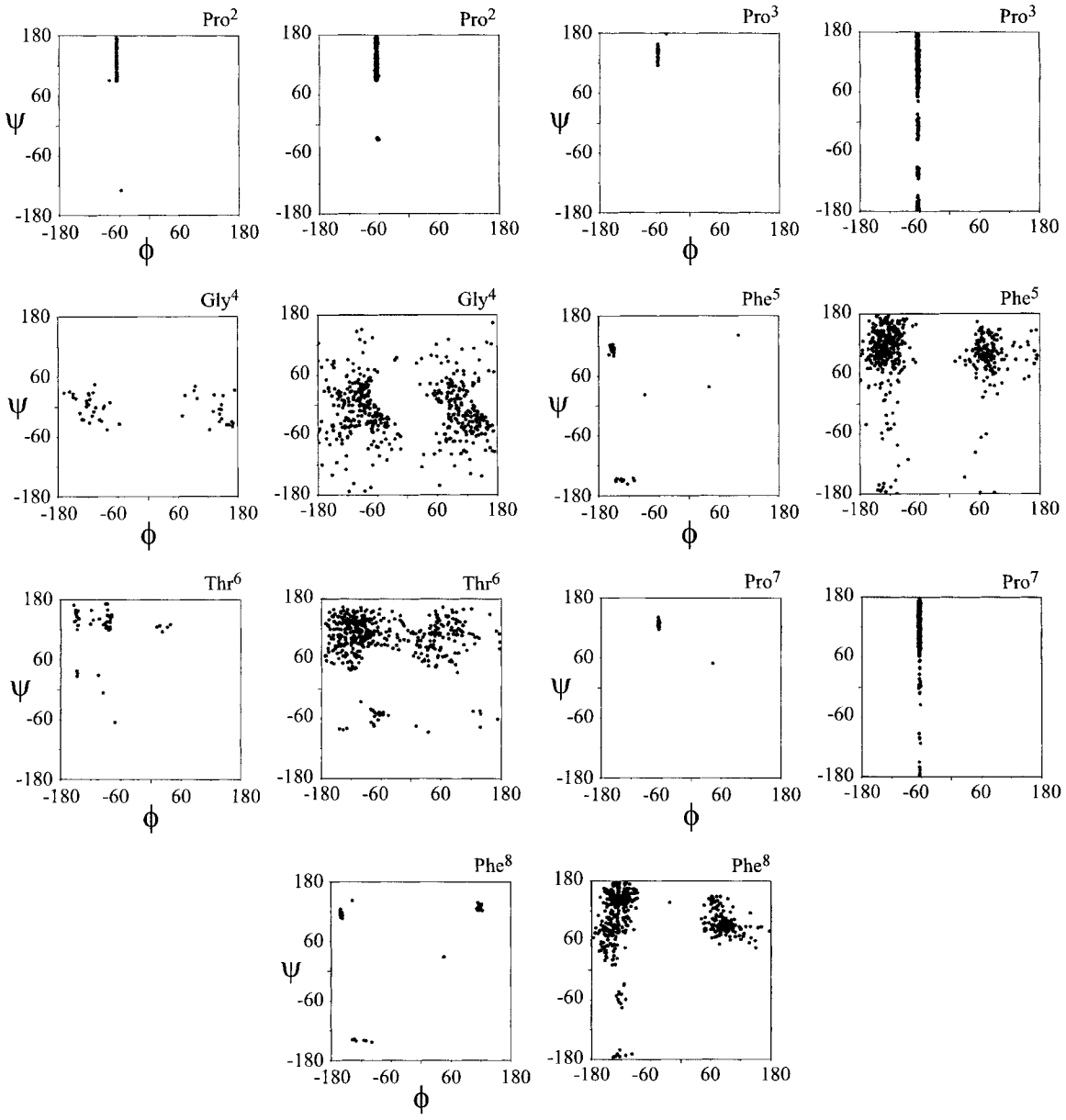

FIGURE 3 Ramachandran maps for the ϕ and ψ dihedral angles of residues 2–8 of (Thr^6)-BK, as obtained from classical DG calculations (on the left) and from ensemble calculations (on the right).

different biological activities of BK and Thr^6-BK to the presence of this turn in the N-terminus. Further investigations to probe this hypothesis are currently underway.

REFERENCES

1. Farmer, S. G. & Burch, R. M. L. R. (1991) in *Bradykinin Antagonists, Basic and Clinical Research,* Burch, R. M., Ed., Marcel Dekker, New York, pp. 1–31.
2. Benetos, A., Gavras, H., Stewart, J. M., Vavrek, R. J., Hatinoglou, S. & Gavras, I. (1986) *Hypertension* **8,** 971–974.
3. Carbonell, L. F., Carreterro, O. A., Stewart, J. M. & Scicli, A. G. (1988) *Hypertension* **11,** 239–243.
4. Regoli, D. & Barabe, J. (1980) *Pharmacol. Rev.* **32,** 1–46.
5. Marceau, F., Lussier, A., Regoli, D. & Giroud, J. P. (1983) *Pharmacology* **14,** 209–229.
6. Steranka, L. R., Manning, D. C., De Haas, C. J., Fer-

kany, J. W., Borosky, S. A., Connor, J. R., Vavrek, R. J., Stewart, J. M. & Snyder, S. H. (1988) *Proc. Natl. Acad. Sci. USA* **85,** 3245–3249.
7. Proud, D., Reynolds, C. J., Lacapra, S., Schotka, A., Lichtenstein, L. M. & Naclerio, R. M. (1988) *Am. Rev. Respir. Dis.* **137,** 613–616.
8. Naclerio, R. M., Proud, D., Lichtenstein, L. M., Sobotka-Kagey, A., Hemdley, J. O., Sorrentino, J. & Gwaltney, J. M. (1988) *J. Infect. Dis.* **157,** 133–142.
9. Kyle, D. J., Martin, J. A., Farmer, S. G. & Burch, R. M. (1991) *J. Med. Chem.* **34,** 1230–1233.
10. Cann, J. R., London, R. E., Matwiyoff, N. A. & Stewart, J. M. (1983) *Am. Exp. Med. Biol.* **156A,** 495–500.
11. Young, J. K. & Hicks, R. P. (1994) *Biopolymers* **34,** 611–623.
12. Mierke, D. F., Geyer, A. & Kessler, H. (1994) *Int. J. Pept. Protein Res.* **44,** 325–331.
13. Lee, S. C., Russel, A. F. & Laidig, W. D. (1990) *Int. J. Peptide Protein Res.* **35,** 367–377.
14. Kyle, D. J., Hicks, R. P., Blake, P. R. & Klimowski, V. J. (1991) in *Bradykinin Antagonists, Basic and Clinical Research,* Burch, R. M., Ed., Marcel Dekker, New York, pp. 131–146.
15. Kyle, D. J., Martin, J. A., Burch, R. M., Carter, J. P., Lu, S., Meeker, S., Prosser, J. C., Sullivan, J. P., Togo, J., Noronha-Blob, L., Sinsko, J. A., Walters, R. F., Whaley, L. W. & Hiner, R. N. (1991) *J. Med. Chem.* **34,** 2649–2653.
16. Kyle, D. J., Martin, J. A., Farmer, S. G. & Burch, R. M. (1991) *J. Med. Chem.* **34,** 1230–1233.
17. Kyle, D. J., Green, L. M., Blake, P. R., Smithwick, D. & Summers, M. F. (1992) *Peptide Res.* **5,** 206–209.
18. Chakravarty, S., Wilkins, D. & Kyle, D. J. (1993) *J. Med. Chem.* **36,** 2569–2571.
19. Kyle, D. J., Blake, P. R., Smithwick, D., Green, L. M., Martin, J. A., Sinsko, J. A. & Summers, M. F. (1993) *J. Med. Chem.* **36,** 1450–1460.
20. Cann, J. R., Liu, X., Stewart, J. M., Gera, L. & Kotovych, G. (1994) *Biopolymers* **34,** 869–878.
21. Pellegrini, M., Mammi, S., Gobbo, M., Rocchi, R. & Peggion, E. (1995) *Biopolymers* **36,** 461–472.
22. Liu, X., Stewart, J. M., Gera, L. & Kotovych, G. (1993) *Biopolymers* **33,** 1237–1247.
23. Guba, W., Haessner, R., Breiphol, G., Henke, S., Knolle, J., Santagada, V. & Kessler, H. (1994) *J. Am. Chem. Soc.* **116,** 1042–1049.
24. Piek, T., Buitenhuis, A., Simon Thomas, R. T. & Ufkes, J. G. R. (1983) *Comp. Biochem. Physiol.* **75C,** 145–152.
25. Piek, T. (1991) *Toxicon* **29,** 139–149.
26. Hue, B. & Piek, T. (1988) in *Neurotox '88, Molecular Basis of Drugs and Pesticide Action,* Lunt, G. G., Ed., Elsevier, Amsterdam, chap. 2, p. 27.
27. Hue, B. & Piek, T. (1989) *Comp. Biochem. Physiol.* **93C,** 87–89.
28. Gobbo, M., Biondi, L., Filira, F., Piek, T. & Rocchi, R. (1995) *Int. J. Peptide Protein Res.* **45,** 459–465.
29. Rance, M., Sørensen, O. W., Bodenhausen, G., Wagner, G., Ernst, R. R. & Wüthrich, K. (1983) *Biochem. Biophys. Res. Commun.* **117,** 458–479.
30. Braunschweiler, L. & Ernst, R. R. (1983) *J. Magn. Reson.* **53,** 521–528.
31. Bax, A. & Davis, D. G. (1985) *J. Magn. Reson.* **65,** 355–360.
32. Jeener, J., Meier, B. H., Bachmann, P. & Ernst, R. R. (1979) *J. Chem. Phys.* **71,** 4546–4553.
33. Macura, S., Huang, Y., Suter, D. & Ernst, R. R. (1981) *J. Magn. Reson.* **43,** 259–281.
34. Drobny, G., Pines, A., Sinton, S., Weitekamp, D. & Wemmer, D. (1979) *Faraday Symp. Chem. Soc.* **13,** 49–55.
35. Bodenhausen, G., Vold, R. L. & Vold, R. R. (1980) *J. Magn. Reson.* **37,** 93–106.
36. States, D. J., Haberkorn, R. A. & Ruben, D. J. (1982) *J. Magn. Reson.* **48,** 286–292.
37. Bothner-By, A. A., Stephens, R. L., Lee, J., Warren, C. D. & Jeanloz, R. W. (1984) *J. Am. Chem. Soc.* **106,** 811–813.
38. Muller, L. (1987) *J. Magn. Reson.* **72,** 191–196.
39. Wüthrich, K., Billeter, M. & Braun, W. (1983) *J. Mol. Biol.* **169,** 949–961.
40. Kim, Y. & Prestegard, J. H. (1989) *J. Magn. Reson.* **84,** 9–13.
41. Havel, T. F. (1991) *Prog. Biophys. Mol. Biol.* **56,** 43–78.
42. Crippen, G. M. & Havel, T. F. (1988) *Distance Geometry and Molecular Conformation,* Research Studies Press, Somerset, England, and John Wiley, New York.
43. Kaptein, R., Boelens, R., Scheek, R. M. & van Gunsteren, W. F. (1988) *Biochemistry* **27,** 5389–5395.
44. Mierke, D. F., Scheek, R. M. & Kessler, H. (1994) *Biopolymers* **34,** 559–563.
45. Wüthrich, K., Billeter, M. & Braun, W. (1984) *J. Mol. Biol.* **180,** 715–740.
46. Reed, J., Hull, W. E., Lieth, C. W., Kubler, D., Subai, S. & Kinzel, V. (1988) *Eur. J. Biochem.* **178,** 141–154.
47. Blanco, F. J., Jiménez, M. A., Rico, M., Santoro, J., Herranz, J. & Nieto, J. L. (1991) *Eur. J. Biochem.* **200,** 345–351.
48. Mierke, D. F., Rudolph-Böhner, S., Müller, G. & Moroder, L. (1995) *Biopolymers* **36,** 811–828.
49. Wilmot, C. M. & Thorton, J. M. (1988) *J. Mol. Biol.* **203,** 221–232.
50. Chou, P. Y. & Fasman, G. D. (1979) *Biophys. J.* **26,** 367–383.
51. Welsh, J. H., Zerbe, O., von Philipsborn, W. & Robinson, J. A. (1992) *FEBS Lett.* **297,** 216–220.
52. Pellegrini, M., Mammi, S., Peggion, E. & Mierke, D. F. (1997) *J. Med. Chem.* **40,** 92–98.